Supporting materials

Evaluating the effects of COVID-19 lockdowns on air quality across some African countries

Zizhen Han[a], Yuqiang Zhang[a*], Zhou Liu[a], Kexin Zhang[b,c], Stanley Numbonui Tasheh[d], Narcisse Tchinda Tsona[a], Zhuyi Wang[a], Bin Luo[a], Likun Xue[a], Xinfeng Wang[a*]

[a] *Environmental Research Institute, Shandong University, Qingdao 266237, China*
[b] *School of Environmental Science and Engineering, Shandong University, Qingdao 266237, China*
[c] *Shenzhen Key Laboratory of Ecological Remediation and Carbon Sequestration, Institute of Environment and Ecology, Tsinghua Shenzhen International Graduate School, Tsinghua University, Shenzhen 518055, China*
[d] *Department of Chemistry, Faculty of Science, The University of Bamenda, P.O Box 39, Bambili, Bamenda, Cameroon*
*Corresponding author. *E-mail address:* yuqiang.zhang@sdu.edu.cn (Y. Zhang), xinfengwang@sdu.edu.cn (X. Wang).

Table S1 Stringency index weighted average of MAM and JJA seasons in major African countries

Country name	Subregion	Season	
		MAM	JJA
Angola	CA	63.22	77.01
Cameroon	CA	52.79	60.04
Central African Rep.	CA	53.28	58.57
Chad	CA	55.32	68.46
Congo	CA	68.67	69.39
Dem. Rep. Congo	CA	64.65	67.12
Gabon	CA	66.88	80.46
Burundi	EA	13.01	12.95
Djibouti	EA	67.95	55.10
Ethiopia	EA	60.98	80.56
Kenya	EA	74.54	80.21
Madagascar	EA	62.94	68.84
Malawi	EA	47.56	61.40
Mozambique	EA	45.20	75.61
Rwanda	EA	71.35	73.72
S. Sudan	EA	63.20	82.16
Somalia	EA	49.13	35.40
Tanzania	EA	39.67	30.43
Uganda	EA	72.72	85.95
Zambia	EA	43.59	48.31
Zimbabwe	EA	67.85	77.02
Algeria	NA	66.86	74.77
Egypt	NA	67.19	75.85
Libya	NA	78.02	92.13
Morocco	NA	78.25	73.64
Sudan	NA	68.54	77.04
Tunisia	NA	74.33	30.29
Botswana	SA	64.94	56.62
eSwatini	SA	70.01	79.65
Lesotho	SA	65.60	64.37
Namibia	SA	55.33	58.20
South Africa	SA	70.33	77.05
Benin	WA	52.05	41.84
Burkina Faso	WA	65.19	29.73
Cote d'Ivoire	WA	61.46	52.38
Gambia	WA	63.56	68.63
Ghana	WA	56.01	56.94
Guinea	WA	60.69	74.46
Liberia	WA	68.87	68.79
Mali	WA	54.14	48.35

Country name	Subregion	Season	
Mauritania	WA	62.97	51.21
Niger	WA	44.35	23.75
Nigeria	WA	65.43	77.58
Senegal	WA	61.87	51.07
Sierra Leone	WA	54.52	43.63
Togo	WA	58.45	52.61

Figure S1: Map showing the study of selected African countries and their subregions. The different colors represent different regions of Africa, namely Northern Africa (NA) is light orange, Western Africa (WA) is green, Central Africa (CA) is orange, Eastern African (EA) is light blue and Southern Africa (SA) is dark blue.
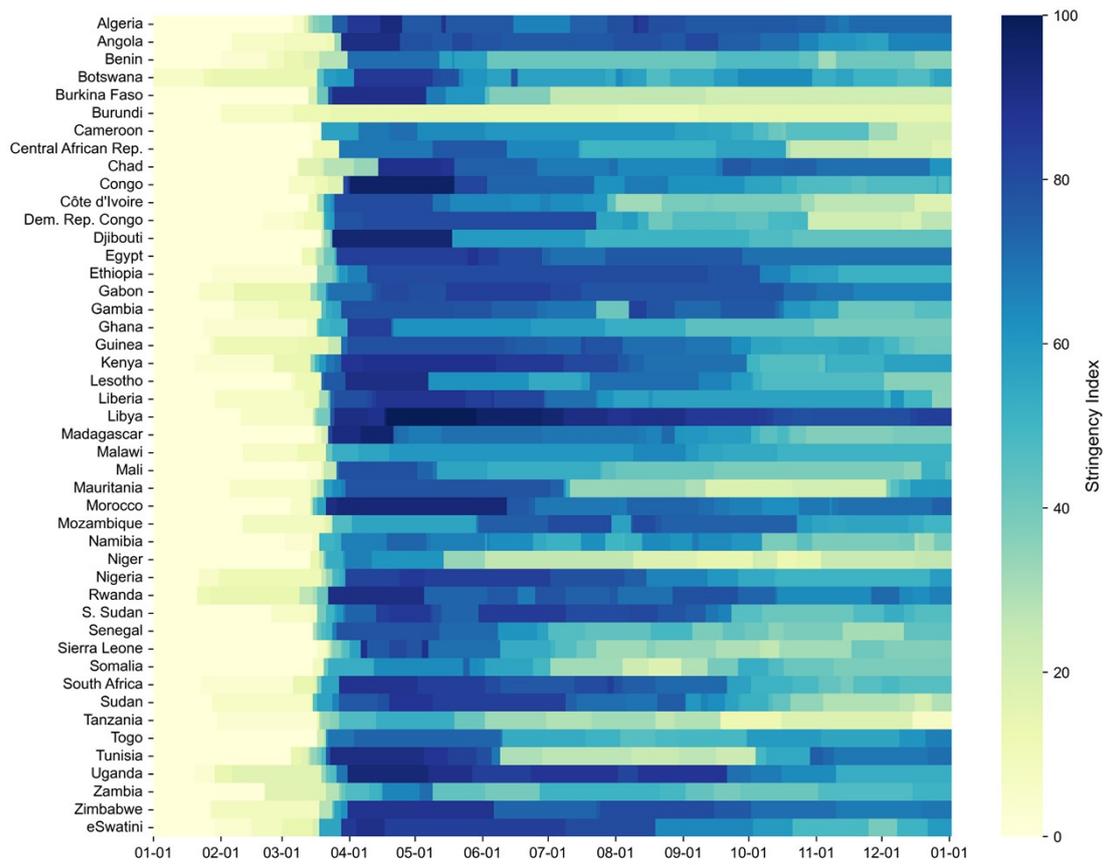
Figure S2: Time distribution of containment stringency index for major African countries in 2020.
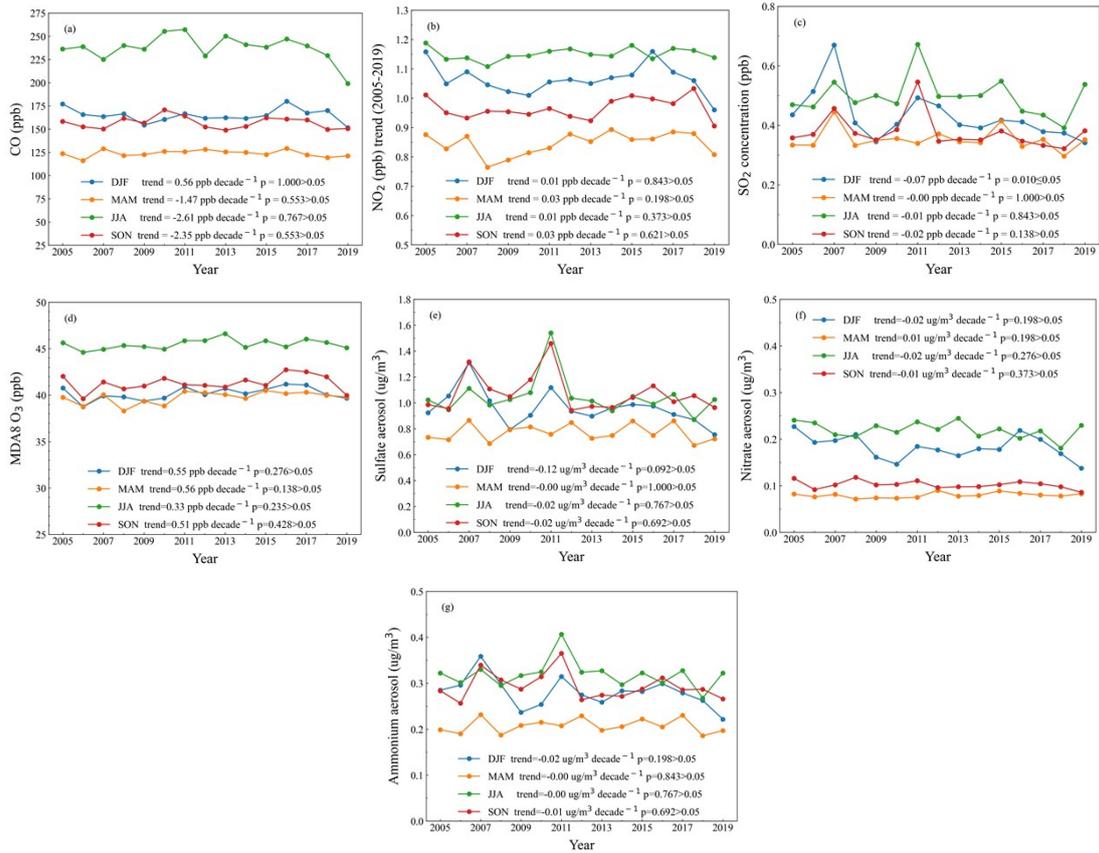
Figure S3: Long-term seasonal air quality trends in Africa from 2005 to 2019 for (a-g) CO, NO$_2$, SO$_2$, MDA8 O$_3$, sulfate aerosol, nitrate aerosol and ammonium aerosol.
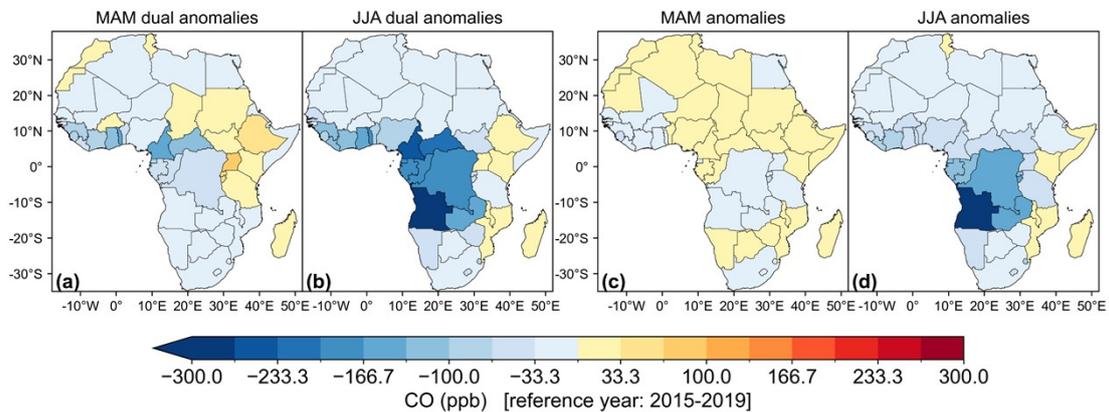
Figure S4: Spatial distribution of CO changes from the two methods: quarterly dual anomalies (a, b), and quarterly anomalies (c, d) for MAM (a, c), JJA (b, d; calculated between 2020 and 5-year average from 2015-2019) in African countries. The units are ppbv.
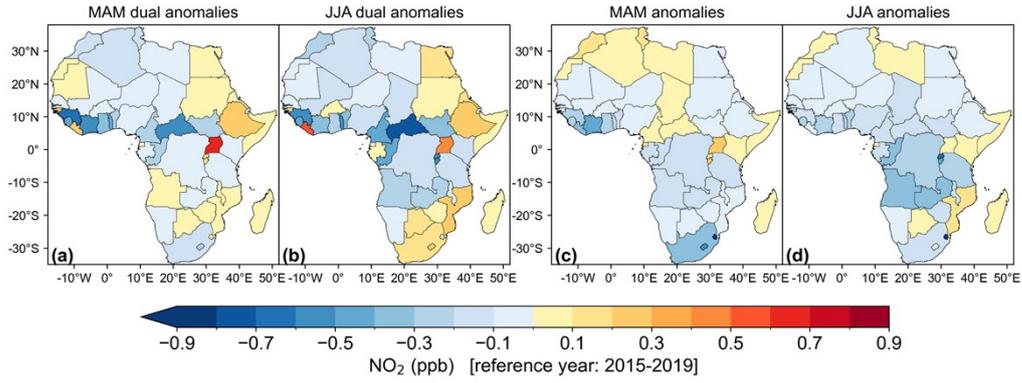
Figure S5: The same as Fig. S4, but for NO₂. The units are ppbv.
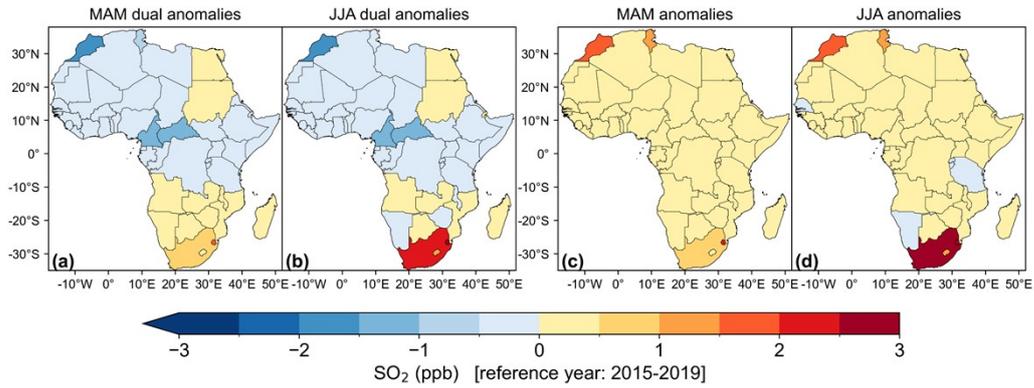
Figure S6: The same as Fig. S4, but for SO₂. The units are ppbv.
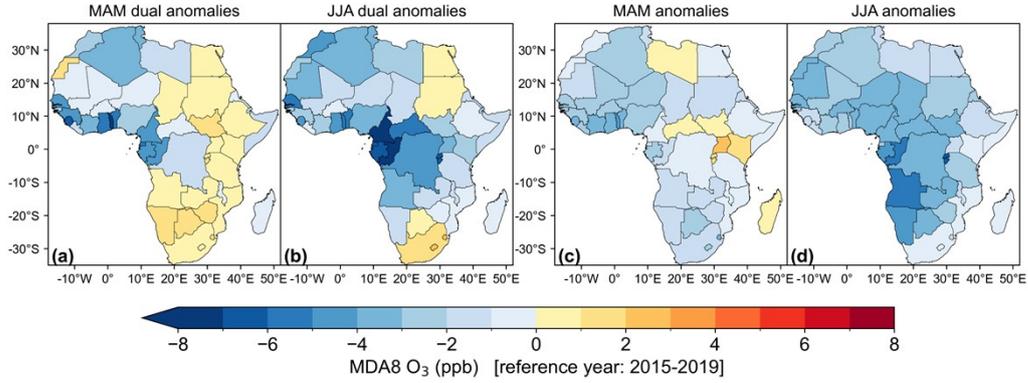
Figure S7: The same as Fig. S4, but for MDA8 O₃. The units are ppbv.
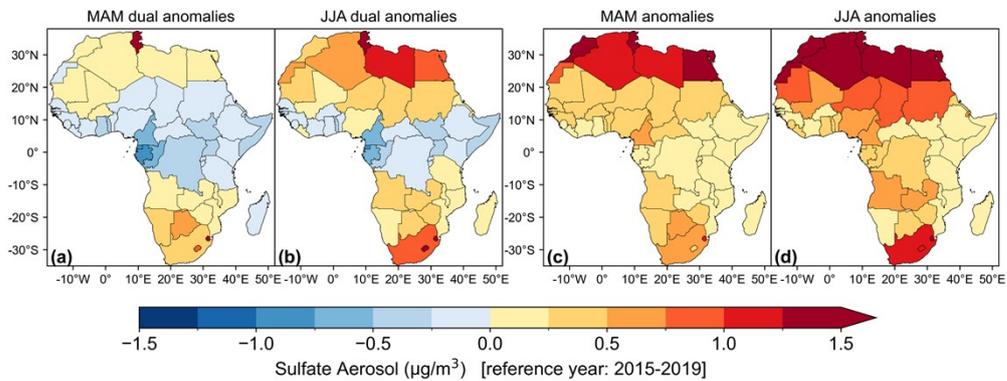
Figure S8: The same as Fig. S4, but for sulfate aerosol. The units are μg/m³.
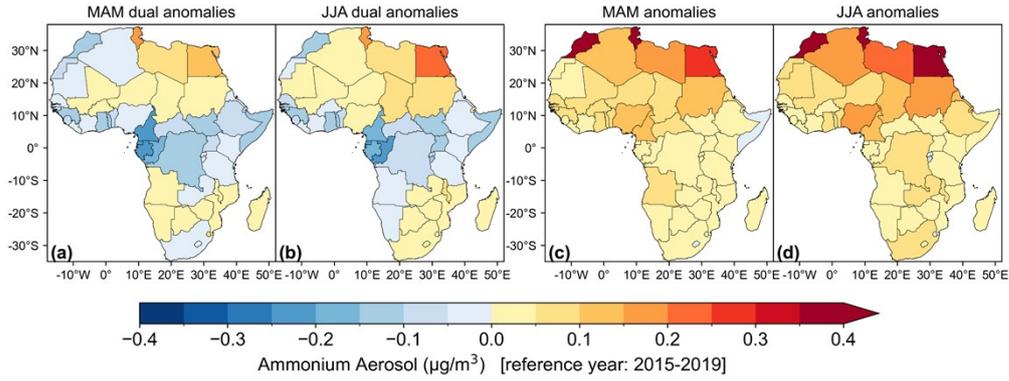
Figure S9: The same as Fig. S4, but for ammonium aerosol. The units are μg/m³.
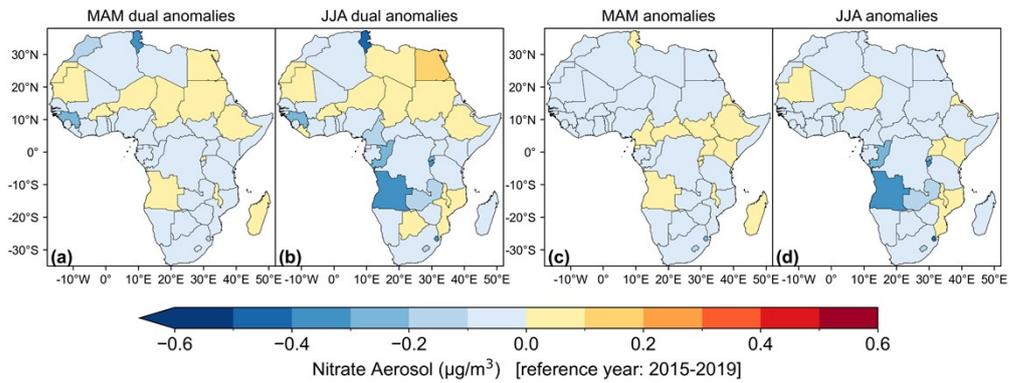
Figure S10: The same as Fig. S4, but for nitrate aerosol. The units are μg/m³.
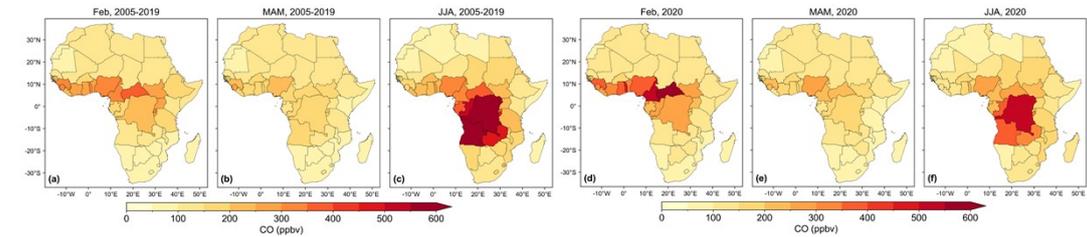
Figure S11: Spatial distribution of CO concentrations in February, MAM, and JJA of previous multiple year average from 2005 to 2019 (a-c), and those in 2020 (d-f).
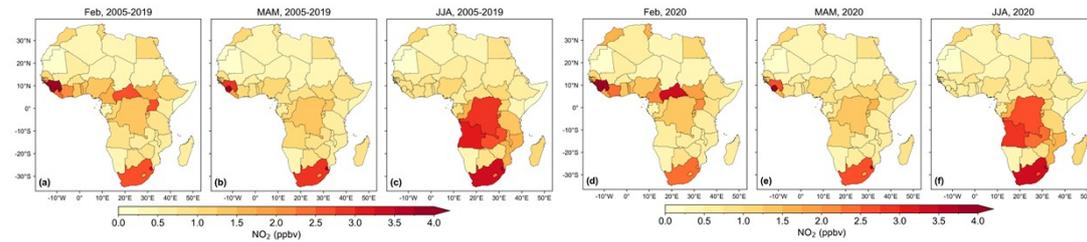
Figure S12: Same as Figure S11, but for NO₂.
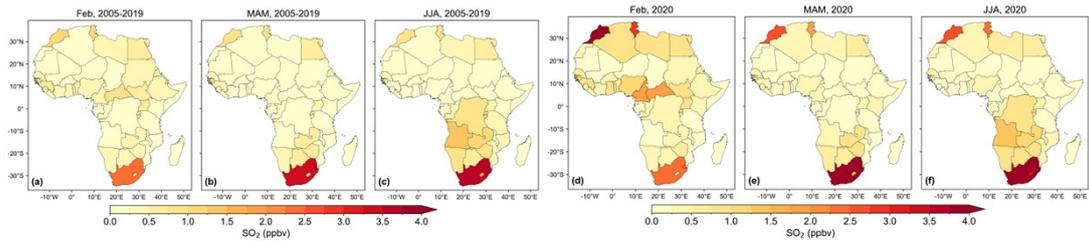
Figure S13: Same as Figure S11 but for SO$_2$.
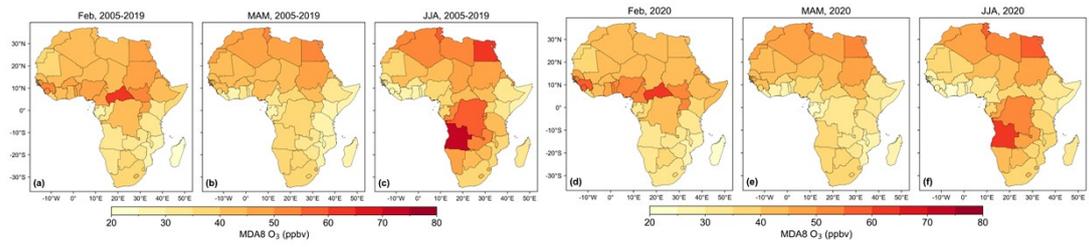
Figure S14: Same as Figure S11, but for MDA8 O$_3$.
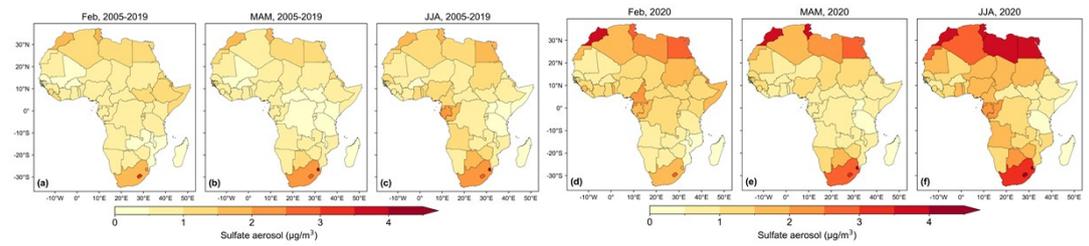
Figure S15: Same as Figure S11, but for sulfate aerosol.
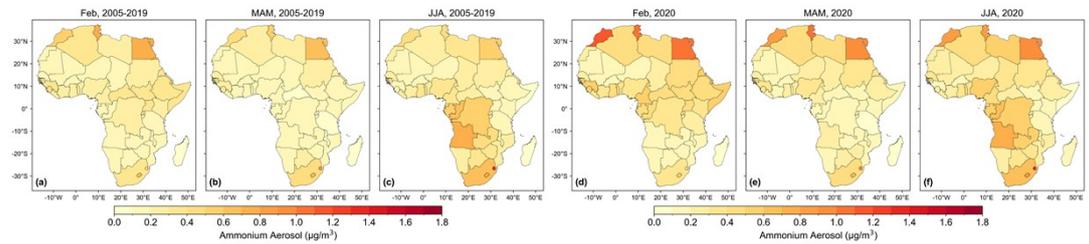
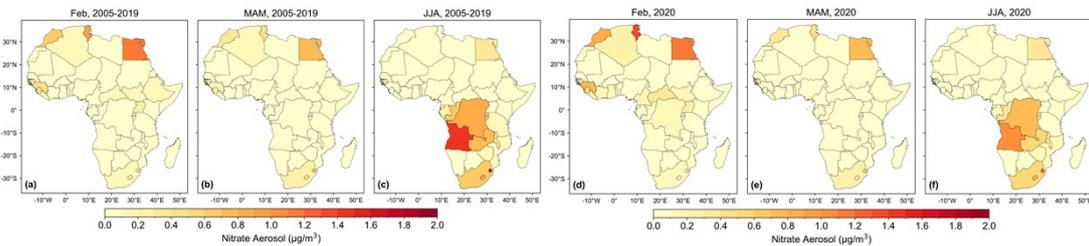**Figure S16: Same as Figure S11, but for ammonium aerosol.**

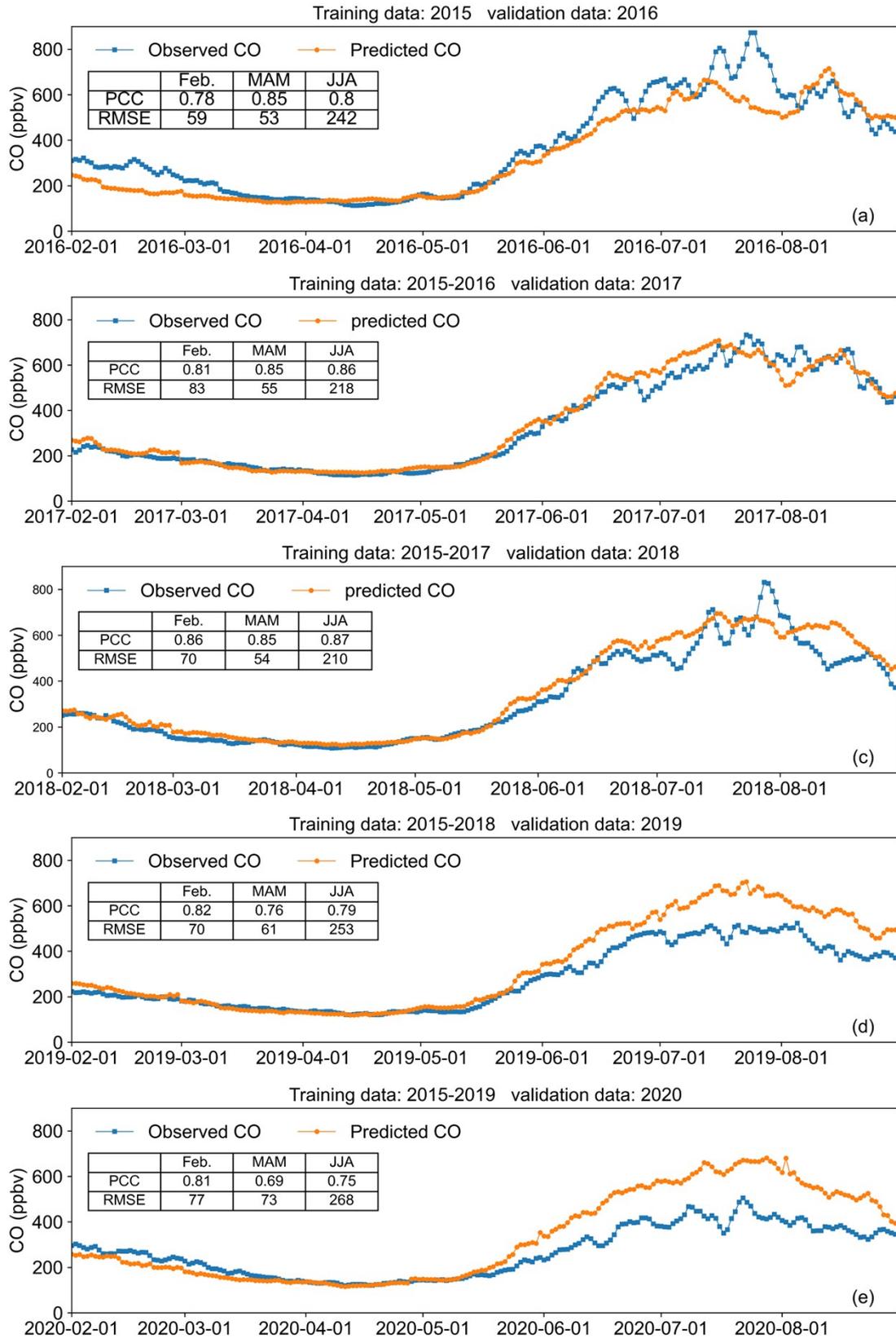**Figure S17: Same as Figure S11, but for nitrate aerosol.**

Figure S18: Time series comparisons between the observed (dashed blue line) and predicted (square orange line) average CO in CA. Figure a-e represents the results of five different time-split sequence validation sets.
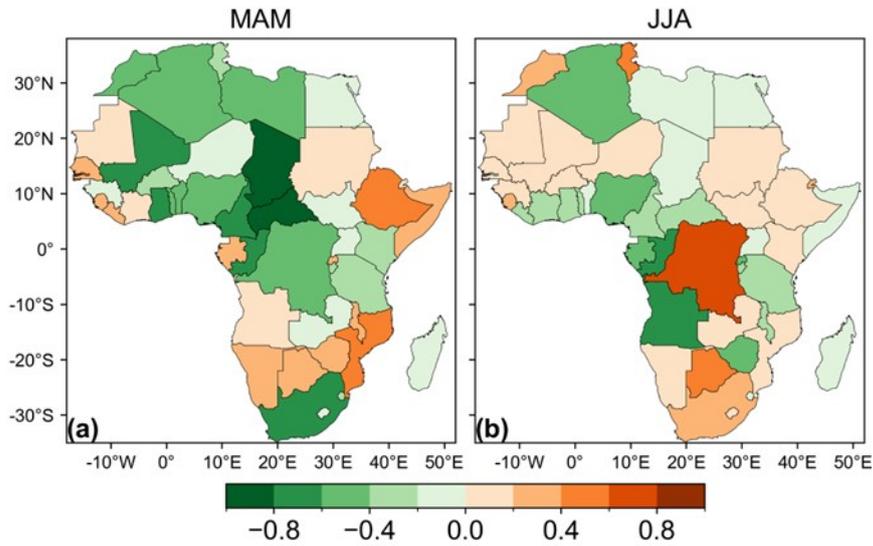
Figure S19: Spatial distribution of Pearson correlation coefficients from March 1st to May 31st (a), and June 1st to August 31st (b) in African countries. Positive values denote positive correlations and negative values denote negative correlations between daily NO$_2$ anomalies and the stringency index.
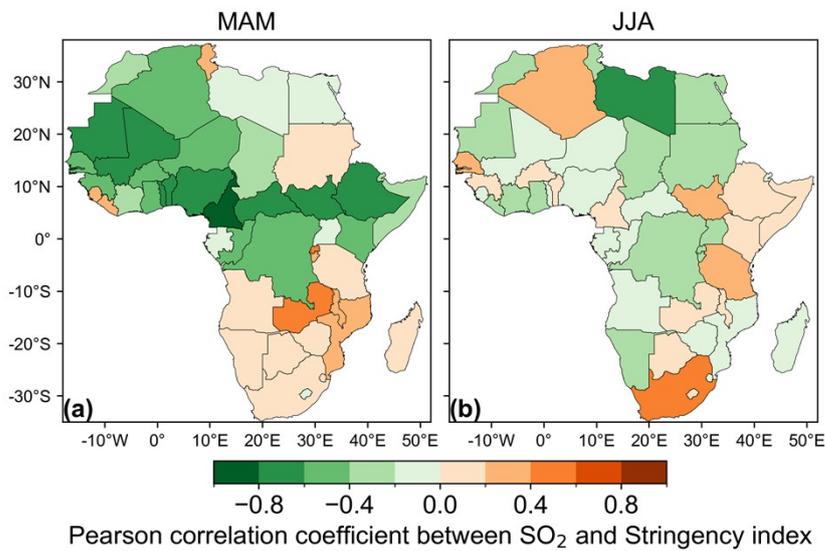

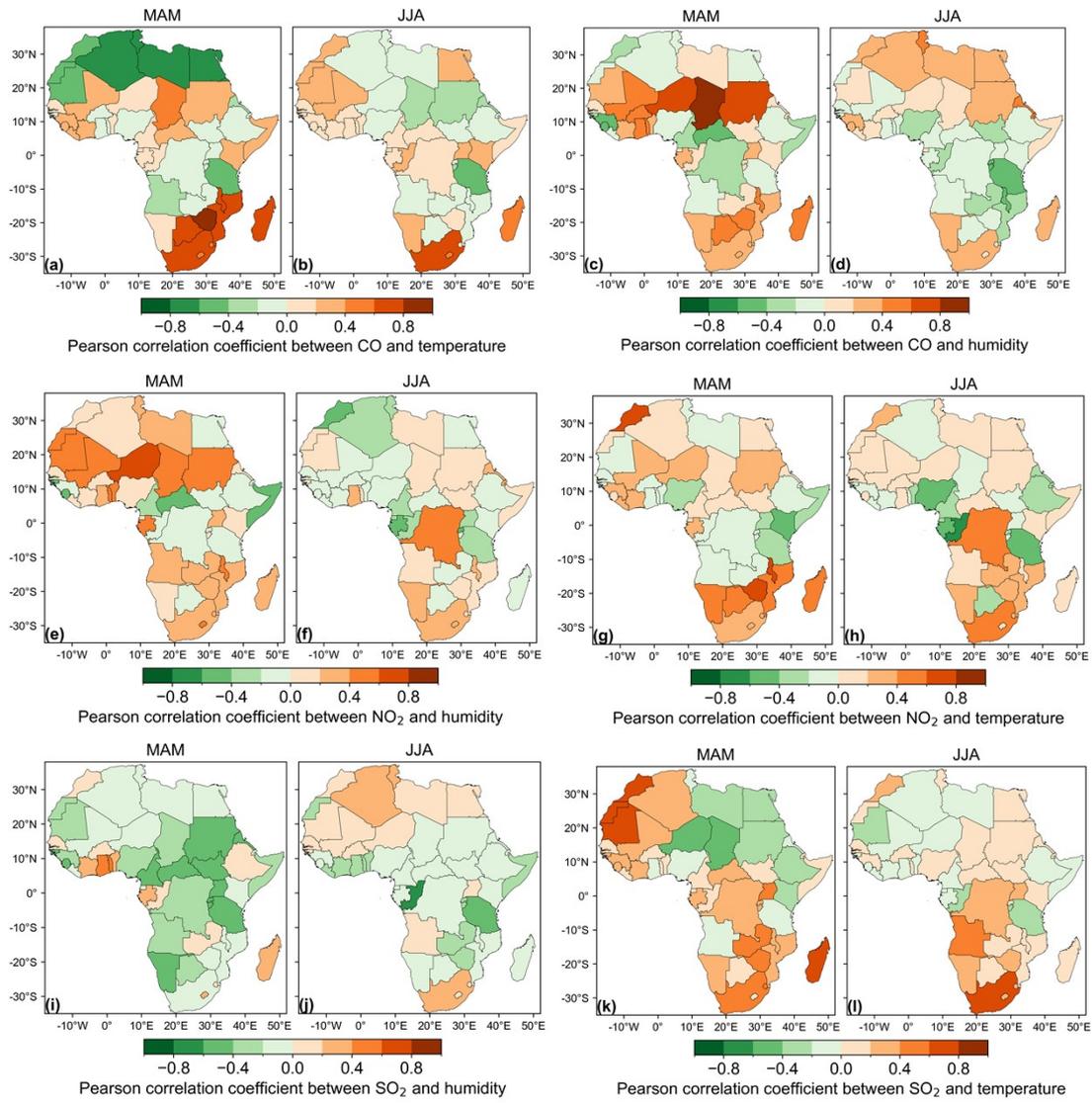**Figure S20: Same as Figure S19, but for SO$_2$.**

Figure S21: Pearson correlation coefficient of (a, b) CO and T, (c, d) CO and humidity, (e, f) NO$_2$ and humidity, (g, h) NO$_2$ and T, (i, j) SO$_2$ and humidity, (k, l) SO$_2$ and T for MAM and JJA in African countries.
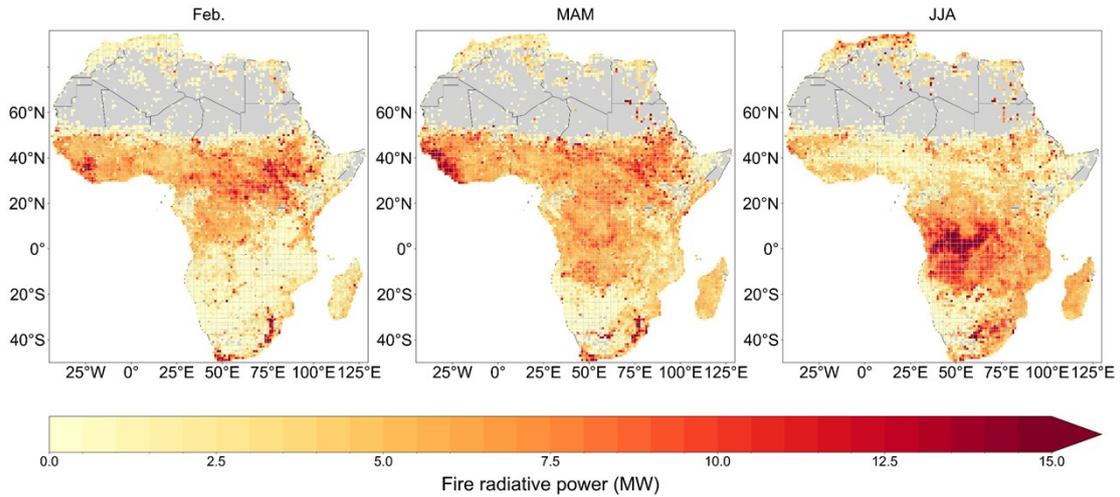
Figure S22: Spatial distribution of average fire radiative power (5-year average from 2015 to 2019) in Feb., MAM and JJA in Africa. Data from the VIIRS-SNPP product, which originates from the Suomi NPP satellite. Data for South Africa, Burkina Faso, cote d'Ivoire, Sierra Leone, W. Sahara and the Central African Republic is missing.
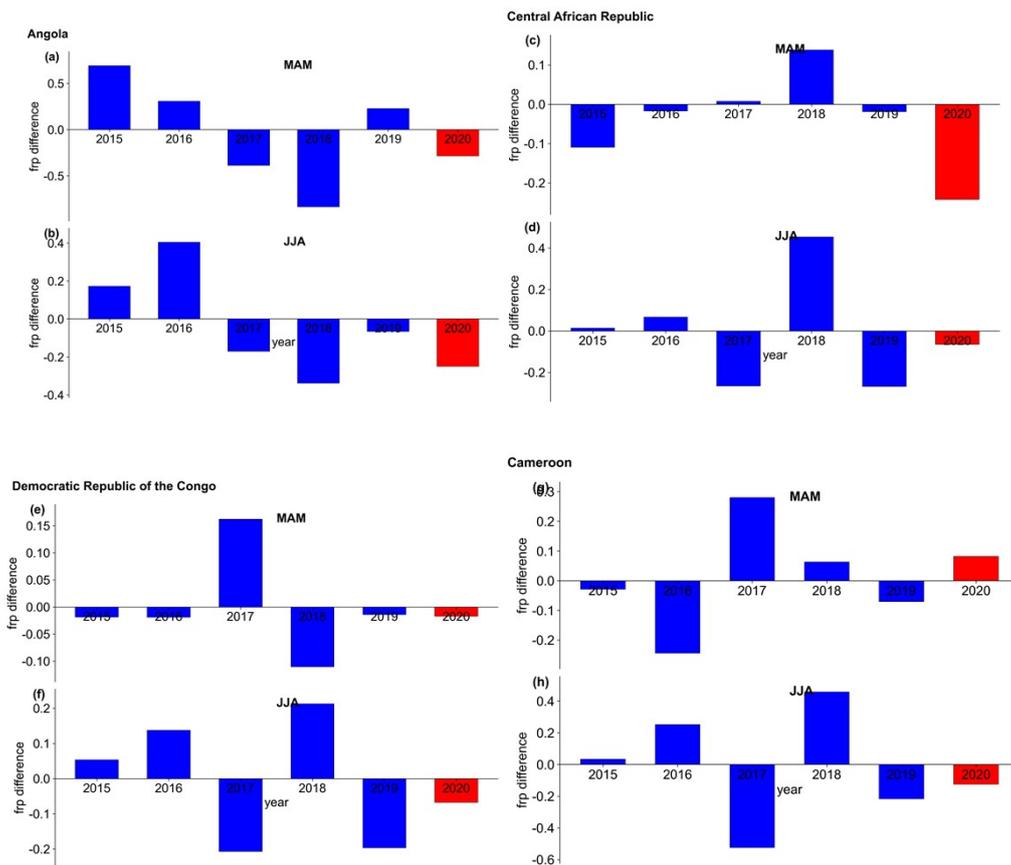

Figure S23: fire radiative power quarterly anomalies (calculated between each year and 5-year average from 2015-2019) in MAM and JJA in (a) Angola, (b) the Central African Republic, (c) the Democratic Republic of the Congo and (d) Cameroon.
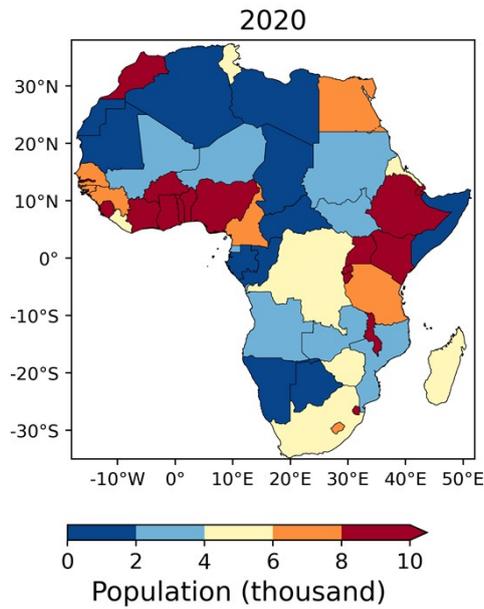
2020

0 2 4 6 8 10
Population (thousand)

Figure S24: Population in 2020 in African countries. Units are thousand. The data from the United Nations.

CO quarterly dual anomalies

CO differences between the RF-predicted and chemical reanalysis

MAM   JJA   MAM   JJA
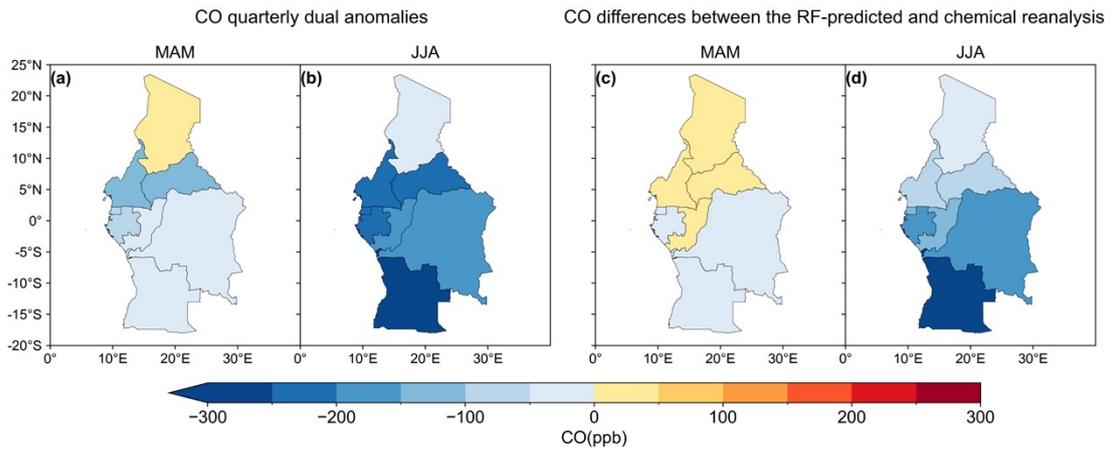
−300   −200   −100   0   100   200   300
CO(ppb)

Figure S25: Spatial distribution of CO quarterly dual anomalies in CA region estimated directly from the chemical reanalysis data (a, b), and the differences between chemical reanalysis and the RF-predicted CO for MAM and JJA in 2020 (c, d). The units are ppbv.
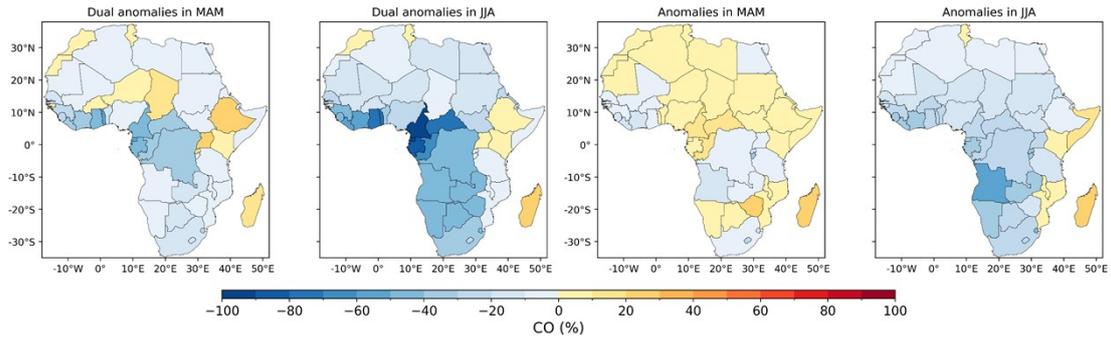
Figure S26: Spatial distribution of CO percentage quarterly dual anomalies (a, b), and percentage quarterly anomalies (c, d; calculated between 2020 and 15-year average from 2005-2019) in MAM and JJA in African countries.
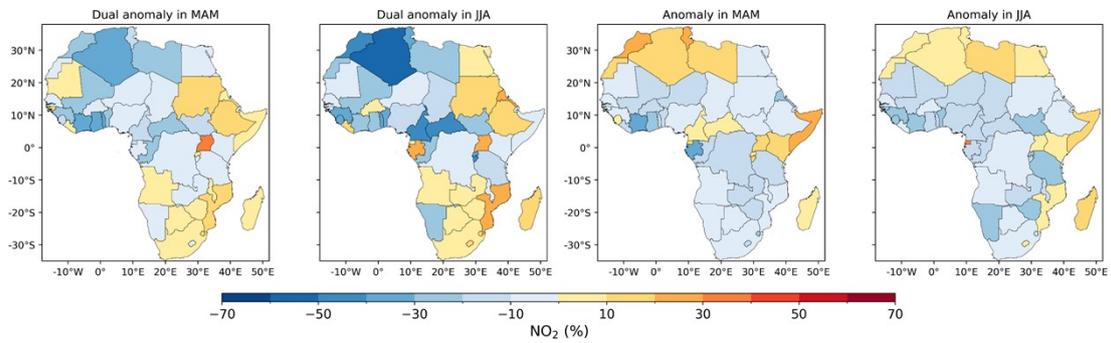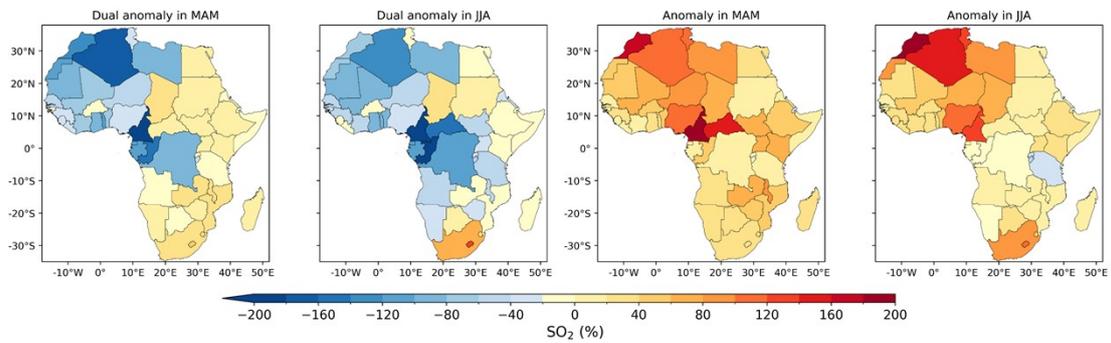

Figure S27: The same as Fig. S26, but for NO$_2$.

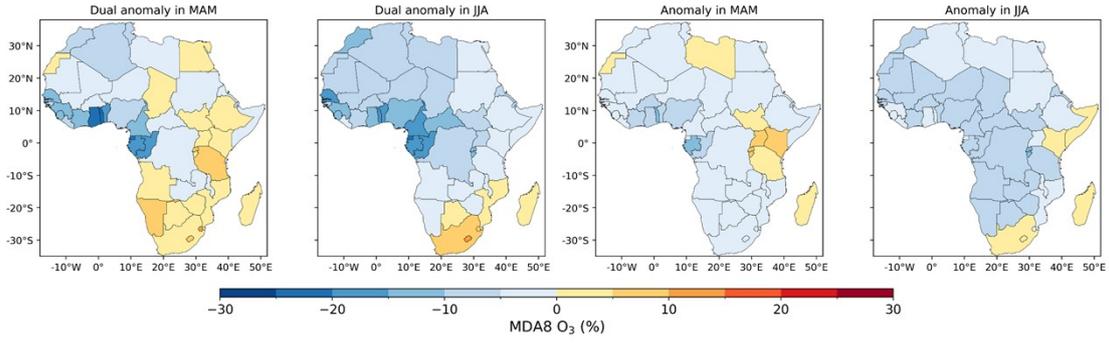**Figure S28: The same as Fig. S26, but for SO$_2$.**

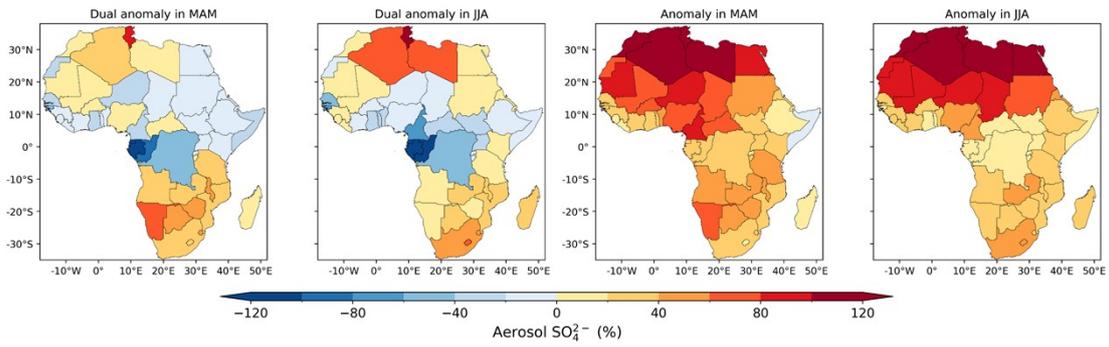**Figure S29: The same as Fig. S26, but for MDA8 O$_3$.**

Figure S30: The same as Fig. S26, but for sulfate aerosol.
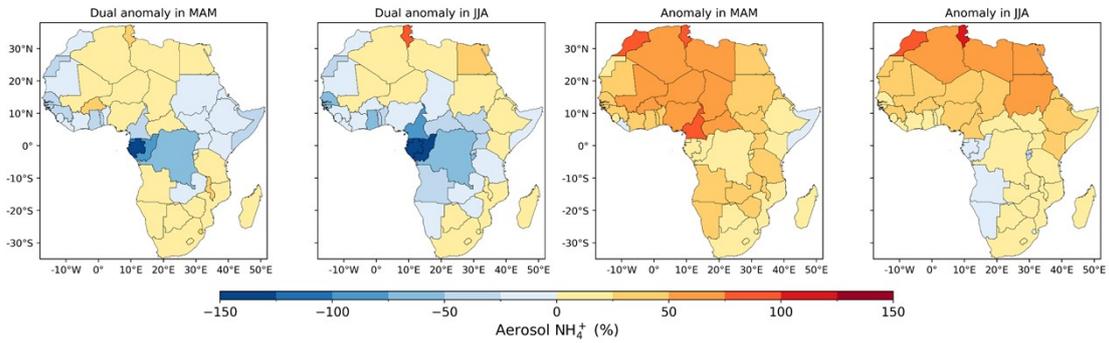

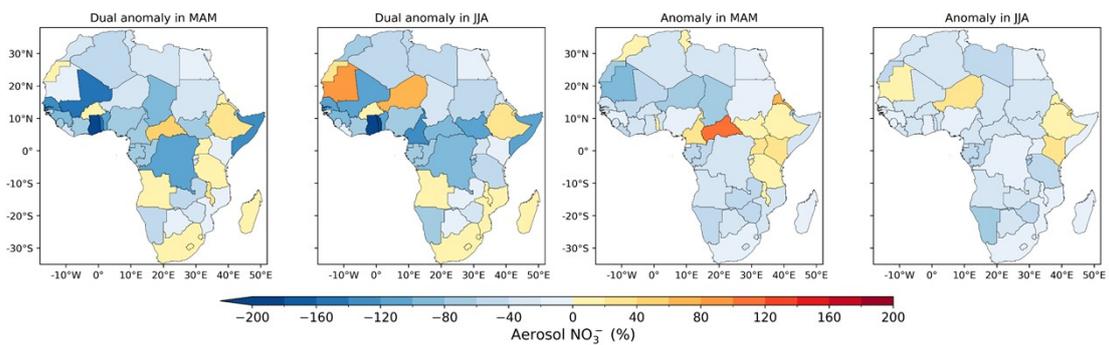**Figure S31: The same as Fig. S26, but for ammonium aerosol.**

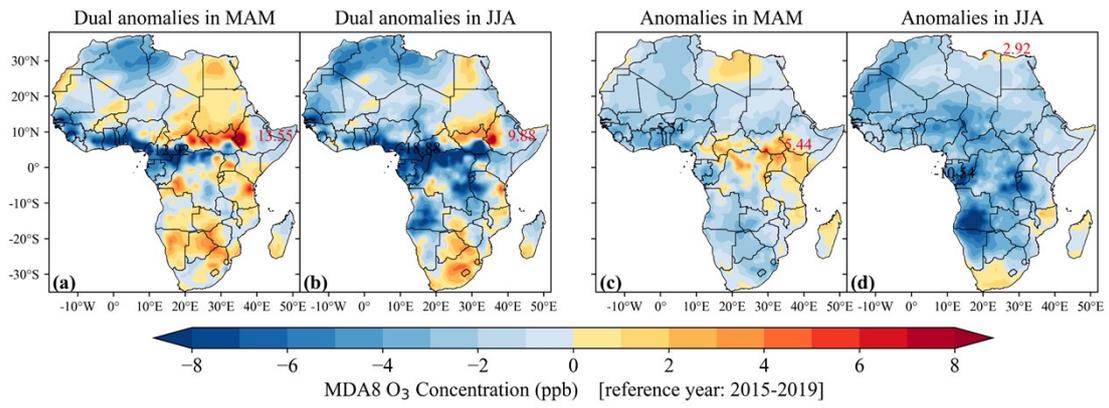**Figure S32: The same as Fig. S26, but for nitrate aerosol.**

Figure S33: Spatial distribution of MDA8 O₃ quarterly dual anomalies (a, b), and quarterly anomalies (c, d) in MAM and JJA in African countries. The differences were calculated between 2020 and 15-year average (2005-2019). The units are ppbv.